Available online at www.sciencedirect.com
ScienceDirect
Ceramics International 35 (2009) 339–344
CERAMICS INTERNATIONAL
www.elsevier.com/locate/ceramint

Sintering behavior and mechanical properties of WC–10Co, WC–10Ni and WC–10Fe hard materials produced by high-frequency induction heated sintering

In-Jin Shon [a,*], In-Kyoon Jeong [a], In-Yong Ko [a], Jung-Mann Doh [b], Kee-Do Woo [a]

[a] *Department of Advanced Materials Engineering, The Research Center of Advanced Materials Development, Chonbuk National University, Chonbuk 561-756, Republic of Korea*
[b] *Advanced Functional Materials Research Center, Korea Institute of Science and Technology, P.O. Box 131, Cheongryang, Seoul 136-791, Republic of Korea*

Received 1 October 2007; received in revised form 19 October 2007; accepted 3 November 2007
Available online 1 February 2008

Abstract

The comparison of sintering behavior and mechanical properties of WC–10 wt.%Co, WC–10 wt.%Ni and WC–10 wt.%Fe hard materials produced by high-frequency induction heated sintering (HFIHS) method was accomplished using ultra-fine powder of WC and binders (Co, Ni, Fe). The advantage of this process allows very quick densification to near theoretical density and prohibition of grain growth in nano-structured materials. Highly dense WC–10Co, WC–10Ni and WC–10Fe with a relative density of up to 99% could be obtained with simultaneous application of 60 MPa pressure and induced current within 1 min without significant change in grain size. The hardness and fracture toughness of the dense WC–10Co, WC–10Ni and WC–10Fe composites produced by HFIHS were investigated.

Keywords: Rapid sintering; High-frequency induction heated sintering; Hard materials; Fracture toughness

1. Introduction

Tungsten carbide hard materials are widely used for a variety of machining, cutting, drilling and other applications. Morphologically, they consist of a high volume fraction of the ''hard'' hexagonal WC phase embedded within a soft and tough Co or Ni binder phase [1]. WC–Co and WC–Ni hard materials can be densified by liquid phase sintering and the mechanical properties of these materials depend on their composition and microstructure (especially on the grain size of the carbide phase [2]). Thus, the control of grain growth of the carbide phase during liquid phase sintering is an important objective. However, cobalt is not economically attractive and the resulted cemented carbide has a low corrosion resistance [3]. This has prompted considerable effort to find a satisfactory alternative binder [4–6]. The focus on Ni as a binder has been motivated by results showing a higher corrosion and oxidation resistance [3]. However, the mechanical properties (hardness and toughness) for WC–Ni are relatively lower than those of WC–Co [6]. The corrosion and oxidation resistance of Fe binder is inferior to that of Co and Ni but is cheaper than Co and Fe.

In general, decreasing WC particle size increases such mechanical properties as hardness, wear resistance and transverse rupture strength of the composites [7]. Increasing the volume fraction of binder increases the fracture toughness at the expense of hardness and wear resistance [8,9]. WC–cobalt and other similar cemented carbides are used as cutting tools because of a combination of desirable high hardness and high fracture toughness because of the respective contributions of the carbide and metallic phases. Densification of WC–Co has been accomplished by conventional sintering [10,11], by sintering in a spark plasma sintering (SPS) apparatus or plasma pressure compaction apparatus [12,13] and by sintering by dynamic shock compression [14]. The primary concern in all these methods is in the grain size of the WC component,

* Corresponding author. Tel.: +82 63 270 2381; fax: +82 63 270 2386.
E-mail address: ijshon@chonbuk.ac.kr (I.-J. Shon).

0272-8842/$34.00
doi:10.1016/j.ceramint.2007.11.003

because it has been established that significant improvements in the mechanical properties can be attained with finer grain size [15,16].

Nanocrystalline materials have received much attention as advanced engineering materials with improved physical and mechanical properties [11,12]. As nano-materials possess high strength, high hardness and excellent ductility and toughness, undoubtedly, more attention has been paid for the application of nano-materials [17,18]. In recent days, nanocrystalline WC–Co cemented carbides have been developed by the thermochemical and thermomechanical process named as the spray conversion process (SCP) [19]. The advantage of SCP is that the WC particle size can be reduced below 100 nm. However, the WC grain size in sintered WC–Co cemented carbides becomes much larger than that in pre-sintered powders due to a fast diffusion through liquid phase during conventional liquid phase sintering process. Therefore, even though the initial WC size is less than 100 nm, the grain size increases rapidly up to 500 nm or larger during the conventional liquid phase sintering [20]. Even though the grain growth inhibitors were added in WC–Co, the WC grains size increases up to 300 nm during the liquid phase sintering process [2,21,22]. So, controlling grain growth during sintering is one of the keys to the commercial success of nano-structured WC, WC–Co and WC–Ni composites. And recently the high-frequency induction heated sintering (HFIHS) technique has been shown to be effective in the sintering of nano-structured materials in very short times (within 1 min) [23,24].

In this work, we report results on the sintering of WC–10 wt.%Co, WC–10 wt.%Ni and WC–10 wt.%Fe by a rapid sintering process, HFIHS, a method which combines induced current with high-pressure application. The goal of this work is to produce dense, ultra-fine WC–10 wt.%Co, WC–10 wt.%Ni and WC–10 wt.%Fe hard materials in very short sintering times (<1 min). And we investigated the effect of binder on the sintering behavior and mechanical properties of WC hard materials.

2. Experimental procedure

The tungsten carbide powder used in this research was supplied by TaeguTec Ltd. (Taegu, Korea). The powder had a grain size of 0.4 μm measured by FSSS and was reported to be 99.5% pure. Cobalt (~3 μm, 99.7% pure, Sigma–Aldrich), nickel (<2 μm, 99.8% pure, Sigma–Aldrich) and iron (<10 μm, 99.9% pure, Alfa) were used as binder materials. Three different compositions were investigated: WC–10 wt.%Co, WC–10 wt.%Ni and WC–10 wt.%Fe. Scanning electron microscope (SEM) images of the starting powders are shown in Fig. 1. Three different compositions with WC–10 wt.%Co, WC–10 wt.%Ni and WC–10 wt.%Fe were investigated. As can be seen from Fig. 1, all the powder grains are generally round and WC exhibit some agglomeration. Tungsten carbide and binder powders (Co, Ni, Fe) were milled in a Universal Mill with a ball-to-powder weight ratio of 6:1. Milling was done in polyethylene bottles using zirconia balls and was performed at a horizontal rotation velocity of 300 rpm for 24 h.

The mixed powders were placed in a graphite die (outside diameter, 45 mm; inside diameter, 20 mm; height, 40 mm) and then introduced into the high-frequency induction heated sintering system made by Eltek Co. in Republic of Korea.

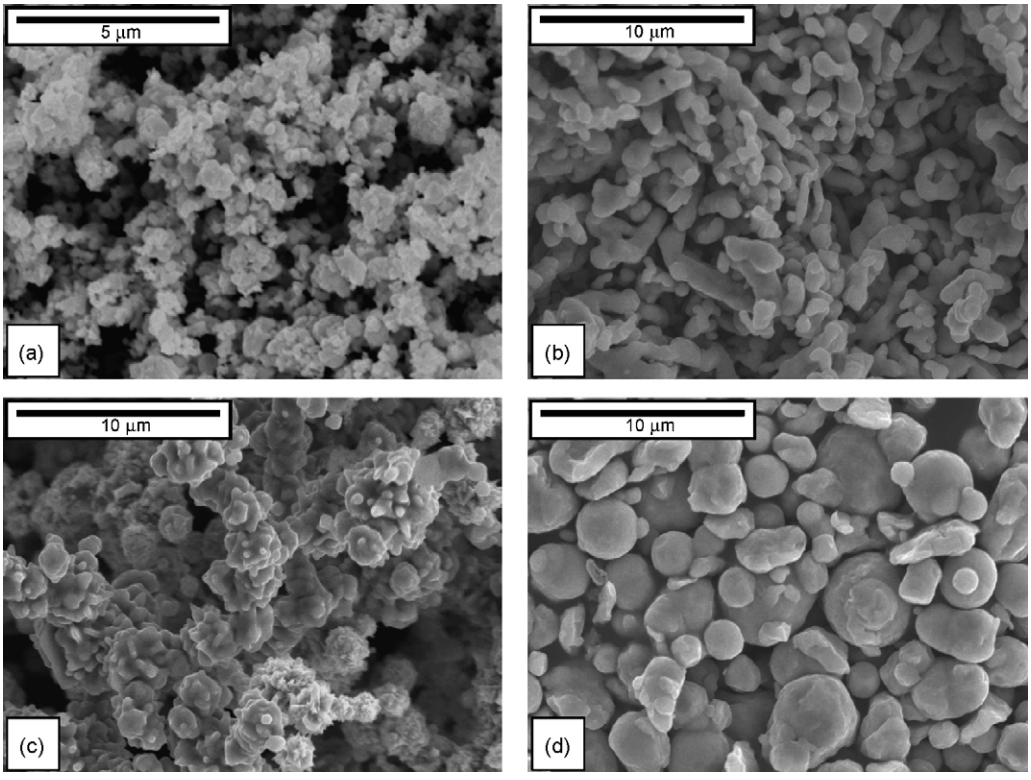

Fig. 1. Scanning electron microscope images of raw materials: (a) tungsten carbide powder, (b) cobalt powder, (c) nickel powder and (d) iron powder.

Schematic diagram of this method is shown in Fig. 2. The system was first evacuated and a uniaxial pressure of 60 MPa was applied. An induced current (frequency of about 50 kHz) was then activated and maintained until the densification rate was negligible, as indicating by the observed shrinkage of the sample. Sample shrinkage is measured in real time by a linear gauge measuring the vertical displacement. The induced current was 90% output of the total power capacity. Temperatures were measured by a pyrometer focused on the surface of the graphite die. Depending on heating rate, the electrical and thermal conductivities of the compact and on its relative density, a difference in temperature between the surface and the center of the sample exists. The heating rates were approximately 2000 °C/min in the process. At the end of the process, the current was turned off and the sample was allowed to cool to room temperature. The entire process of densification using the HFIHS technique consists of four major control stages. These are chamber evacuation, pressure application, power application and cool down. The process was carried out under a vacuum of 4×10^{-2} Torr.

The relative densities of the sintered samples were measured by the Archimedes method. Microstructural information was obtained from product samples, which had been polished and etched, using Murakami's reagent (10 g potassium ferricyanide, 10 g sodium hydroxide and 100 ml water), for 1–2 min at room temperature. Compositional and microstructural analyses of the products were made through X-ray diffraction (XRD), scanning electron microscopy (SEM) with energy dispersive spectroscopy (EDS) and field-emission scanning electron microscopy (FE-SEM). Vickers hardness was measured by performing indentations at a load of 30 kgf and a dwell time of 15 s. The carbide grain size, d_{wc} was obtained by the linear intercept method [25,26].

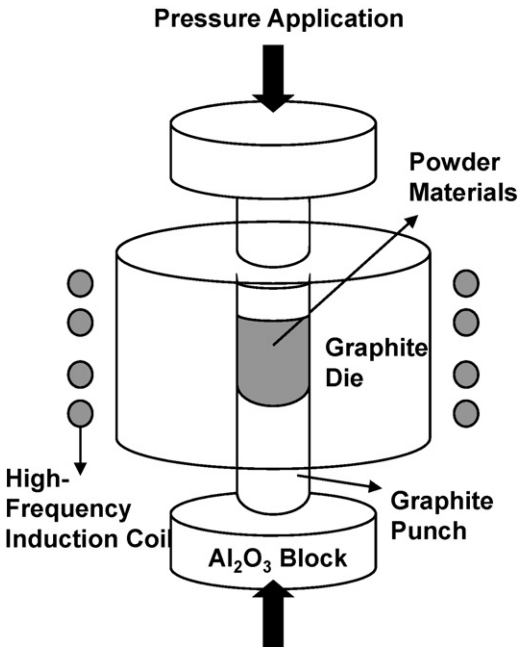

Fig. 2. Schematic diagram of apparatus for high-frequency induction heated sintering.

3. Results and discussion

3.1. Densification behavior and microstructure

The variations of shrinkage and temperature with heating time during the sintering of WC–10 wt.%Co, WC–10 wt.%Ni and WC–10 wt.%Fe by HFIHS under 60 MPa pressure and 90% output of total power capacity are shown in Fig. 3. As the induced current is applied, the shrinkage displacement increased with temperature up to about 950 °C for all cases of WC–10Co, WC–10Ni and WC–10Fe, and then abruptly increased as the temperature is further increased from these values. When the temperature reaches about 1200 °C for the case of WC–Co, WC–Ni and WC–Fe, the densification rate becomes nearly negligible, and as will be seen later, the samples have densified to 98.2%, 99.1% and 99.7% of theoretical density in about 40 s, respectively. In the case of binderless WC hard materials, densification was obtained at about 1600 °C [27]. The densification temperature of WC was reduced remarkably by the addition of Ni, Co and Fe. So it is expected that Co, Ni or Fe would have been molten during the continuation of the sintering. The main densification mechanism for this is carbide particle rearrangement, enhancement of the diffusion and viscous flow of the binder [28]. The nature of the product of sintering is revealed from Fig. 4, which show the XRD patterns of WC–10 wt.%Co, WC–10 wt.%Ni and WC–10 wt.%Fe after sintering. In all cases only peaks belonging to WC are seen, indicating that no compositional changes took place during sintering. Using X-ray mapping, we confirmed the presence of the Co, Ni and Fe.

SEM images of an etched surface of the samples heated to about 1200 °C for the case of WC–Co, WC–Ni and WC–Fe under pressure of 60 MPa in the HFIHS method are shown in Fig. 5. The initially relatively round WC grains became faceted during sintering. The faceting reflects the difference in surface energy of the (0 1 0) and (1 0 0) planes. Because of this anisotropy, WC grains tend to attain a triangular prism shape, as

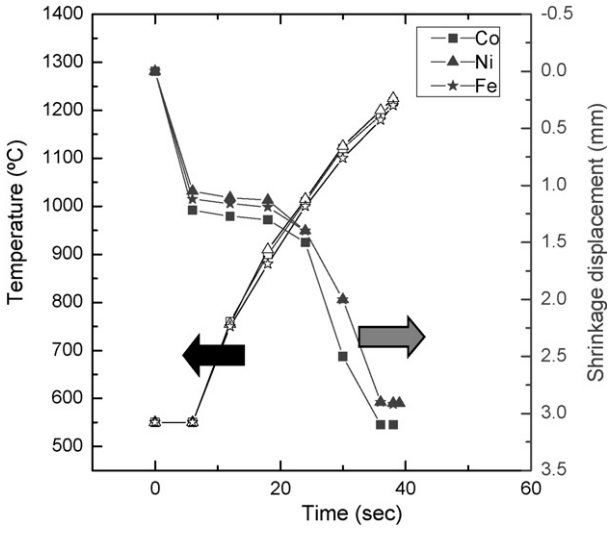

Fig. 3. Variations of temperature and shrinkage displacement with heating time during the sintering of WC–10 wt.%binder hard materials by HFIHS.

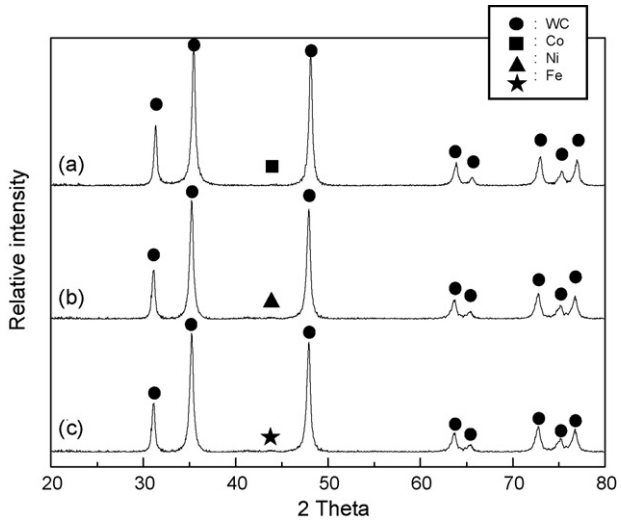

Fig. 4. XRD patterns of (a) WC–10 wt.%Co, (b) WC–10 wt.%Ni and (c) WC–10 wt.%Fe hard materials produced by HFIHS.

has been observed before [29]. The relative densities of WC–10 wt.%Co, WC–10 wt.%Ni and WC–10 wt.%Fe hard materials were about 98.2%, 99.1% and 99.7%, respectively. The attainment of higher density and finer structure in a short time using induction heating with pressure is not well understood. However, we would suggest that the accelerated HFIHS densification may be attributed to a combination of electrical discharge, resistance heating and pressure application effects. When the electric current is applied, energy emission may be concentrated at particle contacts that attain high temperatures. These concentrated heat effects at particle surface may cause surface melting and oxide breakdown, similar to surface effects in the electrodischarge machining (EDM) process [30]. The average sizes of these grains in the nearly fully dense WC–10 wt.%Co, WC–10 wt.%Ni and WC–10 wt.%Fe composites, determined by the linear intercept method, were about 450, 490 and 450 nm, respectively. Thus the fine structure can be obtained without grain growth during the sintering by the HFIHS method.

3.2. Physical and mechanical properties

Vickers hardness measurements were made on polished sections of WC–Co, WC–Ni and WC–Fe composites using a 30 kgf load and 15 s dwell time. Indentations with large enough loads produced radial cracks emanating form the corners of the indent. Fracture toughness was calculated from cracks produced in indentations under large loads. The length of these cracks permits an estimation of the fracture toughness of the material by means of Anstis expression [31].

$$K_{IC} = 0.016\left(\frac{E}{H}\right)^{1/2}\frac{P}{C^{3/2}} \quad (1)$$

where E is Young's modulus, H the indentation hardness, P the indentation load and C the trace length of the crack measured from the center of the indentation. Typically, one to three additional cracks were observed to propagate radially from the indentation. As in the case of hardness values, the toughness values are derived from the average of 10 measurements. The calculated hardness value and fracture toughness value of WC–10Co, WC–10Ni and WC–10Fe made by HFIHS were 10.6 MPa $m^{1/2}$ and 1776 kg/mm^2, 11.1 MPa $m^{1/2}$ and 1750 kg/mm^2, 10.4 MPa $m^{1/2}$ and 1814 kg/mm^2, respectively for 60 MPa and induced current for 90% output of total power capacity. The Vickers hardness and fracture toughness in all WC-based hard materials are similar.

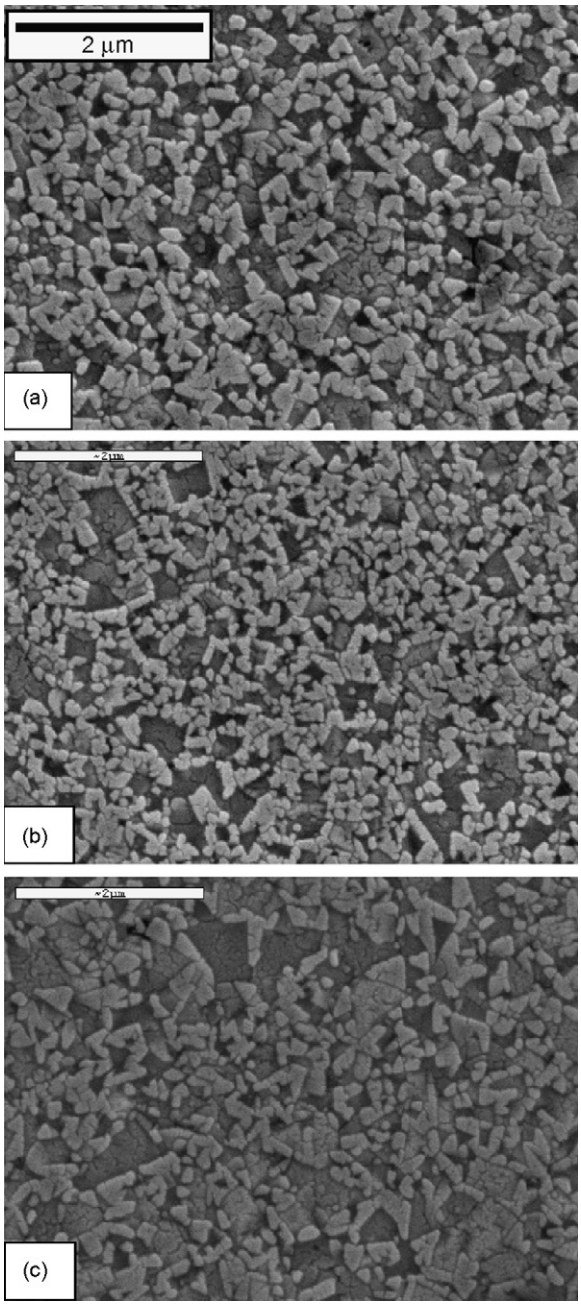

Fig. 5. Scanning electron microscope images of WC–binder hard materials produced by HFIHS: (a) WC–10 wt.%Co, (b) WC–10 wt.%Ni and (c) WC–10 wt.%Fe.

Table 1
Comparison of mechanical properties of WC–10Co, WC–10Ni and WC–10Fe sintered in this study with previously reported values

Reference	Binder content (wt.%)	Relative density (%)	Grain size (μm)	Hv (kg/mm^2)	K_{IC} (MPa m$^{1/2}$)
4	10Co	99.5	1.9	1333	13.5
4	9.6Ni–0.4Co	99.5	1.8	1180	12.5
This work	10Co	98.2	450	1776	10.6
	10Ni	99.1	490	1750	11.1
	10Fe	99.7	450	1814	10.4

Table 1 shows the relative density, grain size, hardness and fracture toughness values obtained in this work and those of comparable cemented carbides reported by others [4]. In the reported study [4], WC–10Co and WC–9.6Ni–0.4Co samples were sintered at 1380 and 1420 °C by conventional methods. The resulting samples had similar grain sizes of approximately 2 μm, which is roughly four times larger than the grain size obtained in this work. Also comparing this investigation (WC–10Co, WC–10Ni and WC–10Fe) with a study of WC–10Co and WC–9.6Ni–0.4Co [4], there is a little difference in fracture toughness, however, a significant difference is seen in hardness values. The hardness of the fine grain WC–10Ni of this study is as much as 50% higher than those of WC–10Co and WC–9.6Ni–0.4Co [4]. These comparisons serve to demonstrate the effect of the grain size. Refinement of the WC grain size improves significantly the hardness of the cemented carbide without decreasing its fracture toughness.

In Table 1, we also compare the mechanical properties between WC–10Co and WC–10Ni hard materials. In both cases, the cermets had WC grains which are about the same in size. As can be seen from Table 1, the use of Ni instead of Co does not suffer from any reduction in mechanical properties. Given the advantage of higher oxidation and corrosion resistance and lower cost for the WC–Ni case, the results are significant for potential applications.

4. Summary

Using high-frequency induction heated sintering, the rapid consolidation of WC–Co, WC–Ni and WC–Fe hard materials were accomplished using ultra-fine powder of WC and binders (Co, Ni, Fe). Nearly fully dense WC–Co, WC–Ni and WC–Fe with a relative density of up to 99% could be obtained with simultaneous application of 60 MPa pressure and induced current within 1 min without significant change in grain size. The grain size of WC in WC–Co, WC–Ni and WC–Fe hard materials were about 450, 490 and 450 nm, respectively. The densification temperature of WC was reduced remarkably by addition of Co, Ni and Fe. The Vickers hardness and fracture toughness of WC–10 wt.%Co, WC–10 wt.%Ni and WC–10 wt.%Fe hard materials are similar.

Acknowledgements

This work was supported by the Korea Science and Engineering Foundation (KOSEF) grant funded by the Korea government (MOST) (No. R01-2007-000-20002-0).

References

[1] K. Mohan, P.R. Strutt, Observation of Co nanoparticle dispersions in WC nanograins in WC–Co cermets consolidated from chemically synthesized powders, Nanostruct. Mater. 7 (5) (1996) 547–555.
[2] B.K. Kim, G.H. Ha, D.W. Lee, Sintering and microstructure of nanophase WC/Co hardmetals, J. Mater. Process. Technol. 63 (1997) 317–321.
[3] S. Imasato, K. Tokumoto, T. Kitada, S. Sakaguchi, Properties of ultra-fine grain binderless cemented carbide 'RCCFN', Int. J. Refract. Met. Hard Mater. 13 (5) (1995) 305–312.
[4] E.A. Almond, B. Roebuck, Identification of optimum binder phase compositions for improved WC hard metals, Mater. Sci. Eng. A 105 (1988) 237–248.
[5] G. Gille, J. Bredthauer, B. Gries, B. Mende, W. Heinrich, Advanced and new grades of WC and binder powder—their properties and application, Int. J. Refract. Met. Hard Mater. 18 (2000) 87–102.
[6] P. Goeuriot, F. Thevenot, Boron as sintering additive in cemented WC–Co (or Ni) alloys, Ceram. Int. 13 (1987) 99–103.
[7] F.L. Zhang, C.Y. Wang, M. Zhu, Nanostructured WC/Co composite powder prepared by high energy ball milling, Scripta Mater. 49 (2003) 1123–1128.
[8] S.G. Shin, Experimental and simulation studies on grain growth in TiC and WC-based cermets during liquid phase sintering, Met. Mater. Int. 6 (2000) 195–201.
[9] M.J. Ledoux, C.H. Pham, J. Guille, H. Dunlop, Compared activities of platinum and high specific surface area Mo_2C and WC catalysts for reforming reactions. I. Catalyst activation and stabilization: reaction of *n*-hexane, J. Catal. 134 (1992) 383–398.
[10] W. Acchar, U.U. Gomez, W.A. Kaysser, J. Goring, Strength degradation of a tungsten carbide–cobalt composite at elevated temperatures, Mater. Charact. 43 (1) (1999) 27–32.
[11] T. Ungar, A. Borbely, Particle-size, size distribution and dislocations in nanocrystalline tungsten–carbide, Nanostruct. Mater. 11 (1) (1999) 103–113.
[12] A. Hirata, H. Zheng, M. Yoshikawa, Adhesion properties of CVD diamond film on binder-less sintered tungsten carbide prepared by the spark sintering process, Diam. Relat. Mater. 7 (1998) 1669–1674.
[13] T.S. Srivatsan, R. Woods, M. Petraroli, T.S. Sudarshan, An investigation of the influence of powder particle size on microstructure and hardness of bulk samples of tungsten carbide, Powder Technol. 122 (2002) 54–60.
[14] K. Yamada, Synthesis of tungsten carbide by dynamic shock compression of a tungsten–acetylene black powder mixture, J. Alloys Compd. 305 (2000) 253–258.
[15] M.S. El-Eskandarany, Structure and properties of nanocrystalline TiC full-density bulk alloy consolidated from mechanically reacted powders, J. Alloys Compd. 305 (2000) 225–238.
[16] L. Fu, L.H. Cao, Y.S. Fan, Two-step synthesis of nanostructured tungsten carbide–cobalt powders, Scripta Mater. 44 (2001) 1061–1068.
[17] K. Niihara, A. Nkahira, Advanced Structural Inorganic Composite, Elsevier Scientific Publishing Co., Trieste, Italy, 1990.
[18] S. Berger, R. Porat, R. Rosen, Nanocrystalline materials: a study of WC-based hard metals, Prog. Mater. Sci. 42 (1997) 311–320.
[19] Z. Fang, J.W. Eason, Study of nanostructured WC–Co composites, Int. J. Refract. Met. Hard Mater. 13 (1995) 297–303.
[20] M. Sommer, W.-D. Schubert, E. Zobetz, P. Warbichler, On the formation of very large WC crystals during sintering of ultrafine WC–Co alloys, Int. J. Refract. Met. Hard Mater. 20 (2002) 41–50.

[21] S.I. Cha, S.H. Hong, B.K. Kim, Spark plasma sintering behavior of nanocrystalline WC–10Co cemented carbide powders, Mater. Sci. Eng. A 351 (2003) 31–38.
[22] S.I. Cha, S.H. Hong, G.H. Ha, B.K. Kim, Microstructure and mechanical properties of nanocrystalline WC–10Co cemented carbides, Scripta Mater. 44 (2001) 1535–1539.
[23] H.C. Kim, I.J. Shon, Z.A. Munir, Rapid sintering of ultra-fine WC–10 wt%Co by high-frequency induction heating, J. Mater. Sci. 40 (2005) 2849–2854.
[24] H.C. Kim, D.Y. Oh, I.J. Shon, Sintering of nanophase WC–15 vol.%Co hard metals by rapid sintering process, Int. J. Refract. Met. Hard Mater. 22 (2004) 197–203.
[25] K. Jia, T.E. Fischer, G. Gallois, Microstructure, hardness and toughness of nanostructured and conventional WC–Co composites, Nanostruct. Mater. 10 (1998) 875–891.
[26] J.H. Han, D.Y. Kim, Determination of three-dimensional grain size distribution by linear intercept measurement, Acta Mater. 46 (1998) 2021–2028.
[27] H.C. Kim, J.K. Yoon, J.M. Doh, I.Y. Ko, I.J. Shon, Rapid sintering process and mechanical properties of binderless ultra fine tungsten carbide, Mater. Sci. Eng. A 435/436 (2006) 717–724.
[28] G.S. Upadhyaya, Materials science of cemented carbides—an overview, Mater. Des. 22 (2001) 483–489.
[29] A.V. Shatov, S.A. Firstov, I.V. Shatova, The shape of WC crystals in cemented carbides, Mater. Sci. Eng. A 242 (1998) 7–14.
[30] J. Fleischer, T. Masuzawa, J. Schmidt, M. Knoll, New applications for micro-EDM, J. Mater. Process. Technol. 149 (2004) 246–249.
[31] G.R. Anstis, P. Chantikul, B.R. Lawn, D.B. Marshall, A critical evaluation of indentation techniques for measuring fracture toughness. I. Direct crack measurements, Am. Ceram. Soc. 64 (1981) 533.